

Wojciech SZYNKIEWICZ, Teresa ZIELIŃSKA, Włodzimierz KASPRZAK

Robotized machining of big work pieces: Localization of supporting heads

© Higher Education Press and Springer-Verlag Berlin Heidelberg 2010

Abstract A planner for a self adaptable and reconfigurable fixture system is proposed. The system is composed of mobile support agents that support thin sheet metal parts to minimize part dimensional deformation during drilling and milling operations. Compliant sheet metal parts are widely used in various manufacturing processes including automotive and aerospace industries. The main role of the planner is to generate an admissible plan of relocation of the mobile agents. It has to find the admissible locations for the supporting heads that provide continuous support in close proximity to the tool and trajectories of the mobile bases characterized by very high speeds during the relocation phases.

Keywords fixture, robot, milling, drilling

1 Introduction

A fixture is a device for locating, constraining, and adequately supporting a workpiece during a manufacturing operation. The fixture procedure, like grasping, seeks arrangements of contacts that restrict the possible motions of a given part. An important factor in fixture design is to optimize the fixture layout, i.e., positions of mobile locators, so that workpiece deformation due to clamping and machining forces is minimized [1,2]. In this paper, we consider that the manufacturing process consists of drilling

and milling (contouring) of thin-sheet aluminium parts for aircrafts and automotive bodies. Workpiece deformation is unavoidable due to its elastic nature, and the external forces impacted by the clamping actuation and machining operations. When severe part displacement is expected under the action of imposed machining forces, supports are needed and should be placed below the workpiece to prevent or constrain deformation.

The existing fixtures for thin-walled workpieces like sheet-metal parts with complex surface geometries are: 1) large mould-like fixtures; 2) modular flexible fixture systems (MFFSs); and 3) single structure flexible fixture systems (SSFFSs). The fixtures traditionally used in manufacturing of thin-sheet metal parts are large moulds reproducing the shape of the skin to be supported; however, this type of fixture is part specific and not reconfigurable. The mould surface is usually equipped with vacuum suction chambers and channels for holding the skin.

MFFSs can be further classified on the basis of their adjusting mechanism: 1) partially reconfigurable with limited number of supports that can be manually relocated; 2) adjusted by separate devices, e.g., robot manipulators; and 3) self-reconfigurable with a matrix of support elements with embedded actuators (in each locator/clamp). It should be noted that all such fixtures still require some human intervention to reconfigure. Various MFFSs have been proposed [3–5]; however, their usage for thin-walled parts fixturing is rather limited. Because fixturing requirements vary during different machining operations required on a single part, it is necessary to reposition the supports, interrupting the production process. MFFSs systems can be adapted to various parts; however, their initial cost is often high when the configuration is complex and time consuming.

One way to avoid this problem is to use an SSFFS of the pin-bed type, with a matrix of supports, which provides support comparable to a mould-like fixture. The main

Received February 28, 2010; accepted April 12, 2010

Wojciech SZYNKIEWICZ, Włodzimierz KASPRZAK
Institute of Control and Computation Engineering, Warsaw University of
Technology, Warsaw 00-665, Poland

Teresa ZIELIŃSKA (✉)

Institute of Aeronautics and Applied Mechanics, Warsaw University of
Technology, Warsaw 00-665, Poland
E-mail: teresaz@meil.pw.edu.pl

disadvantages are high cost and lack of modularity, which makes them difficult or inefficient to use for parts of differing sizes.

Robotic fixtureless assemblies (RFAs) replace traditional fixtures by robot manipulators equipped with grippers that can cooperatively hold the workpiece [6,7]. Using RAFs, different parts can be manufactured within one work-cell and transitions to other workpieces can be done relatively quickly. However, RAFs have their drawbacks such as high complexity, limited number of robots (and thus holding grasps), and high dependence on software.

Proper fixture design is crucial to product quality in terms of precision, accuracy, and surface finish of the machined parts. Therefore, the research devoted to fixture optimization is quite extensive [1,8,9]. Various techniques have been proposed for optimization of fixture layout by formulating different objective functions to determine the location of fixturing supports. In the research for compliant sheet metal parts, Menassa et al. [1] used a finite element model of the workpiece to model the deformation, and determine fixture locations by optimizing an objective that is a function of the deformations at the nodes. The design variables are three fixture locators on primary datum as required by the 3-2-1 principle. In Ref. [10] an optimization algorithm to obtain the optimal number and location of clamps that minimize the deformation of compliant parts is proposed. Cai et al. [8] proposed the N -2-1 fixture layout principle for constraining compliant sheet metal parts. This is used to replace the conventional 3-2-1 principle to reduce deformation of sheet-metal parts. They presented algorithms for finding the best N locating points such that total deformation of a sheet metal is minimized. They used a finite element model of the part with quadratic interpolation, constraining nodes in contact with the primary datum to only in-plane motion. Nonlinear programming was utilized to obtain the optimal fixture layout. DeMeter [9] introduced a fast support layout optimization model to minimize the maximum displacement-to-tolerance ratio of a set of part features subject to a system of machining loads. The speed-up of the optimization is obtained by a reduced stiffness matrix approach. Most of the previous research related to fixture modeling and design considers fixture in static conditions.

The concept described in this paper merges the advantages of RFAs with those of MFFSs, namely, ability to distribute the support action, adaptability to part shapes in a larger range, and high stiffness of the provided support. In our case each fixture element referred to as a physical agent is composed of a mobile robot base, a parallel kinematic machine (PKM) fixed to the mobile platform, an adaptable head with phase-change fluid and an adhesion arrangement, to sustain the supported part perfectly adapting to the part local geometry. The mobility of each support agent and the possibility for the agents to group in regions where some manufacturing operation is

being executed results in higher flexibility with lower number of support agents.

2 Problem formulation — self-adaptable reconfigurable fixture system

A flexible fixture system is composed of mobile robotic agents that can freely move on a bench and reposition below the supported workpiece, without removing the part from the fixture, as shown in Fig. 1. It is assumed that the workpiece is held in position by a subset of locators (not shown in this figure) that remain largely static during the cycle. The remaining agents are highly mobile and change locations to provide additional support in areas affected by the machining process. As mentioned before, each support robot consists of a mobile base, a PKM, and an adaptable head. Two mobile agents alternatively support a thin sheet while a machine tool with a milling cutter contours the workpiece. To simplify motion planning and collision avoidance, the robots are assumed to move along parallel trajectories. Heads adapt to the local geometry of the workpiece to support it at every repositioning. Adaptation is at two levels: head rotation, to match the approximate orientation of the part surface normal, and head surface deformation, to match the local part surface geometry.

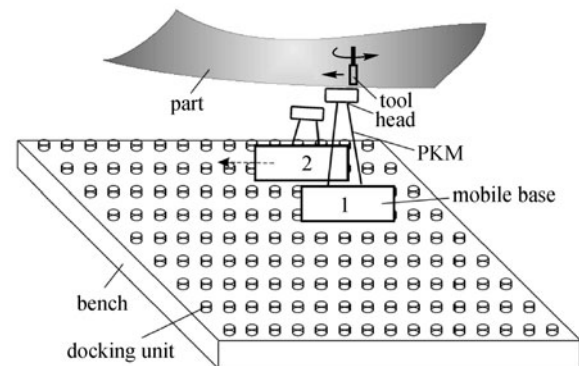


Fig. 1 Self-adaptable reconfigurable fixture system

The overall goal is to develop the planner, which on the basis of CAD geometric data about the workpiece, representing its state before and after machining, will generate the plan of relocation of the mobile bases and the manipulators. Planning process is decomposed into four phases: planning a sequence of admissible head placements, planning a corresponding sequence of mobile platform locations, path planning for mobile platforms and PKMs, trajectory planning for mobile platforms and PKMs (Fig. 2). Obtaining an admissible sequence of head locations is the most difficult part of the planning process. In the paper we present an approach to solve this problem.

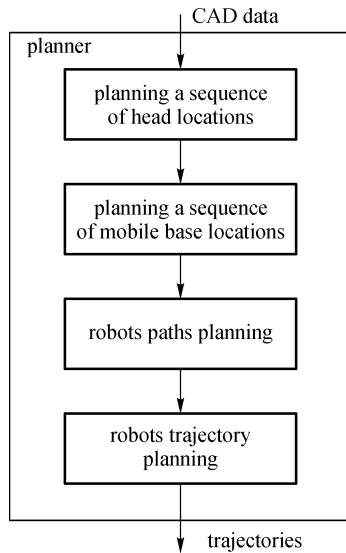


Fig. 2 Planner decomposition

3 Drilling following circular path

3.1 Notation

The following notation will be used: to describe the points and vectors the lower script will be used for quantity indexing, the upper right script marks the reference frame.

The region to be machined is assumed here to be a round hole with some radius r_c . The drilled points are located along an arc and are in constant distance from the edge of the hole, while the milling is performed along the edge of the hole. Depending on machining operation, the value of r , marking the radius of drilled or milled arc, can appropriately differ. The points for drilling are distributed evenly, the internal angle marked by consecutive drilling points is α .

We introduce two reference frames:

1) Moving frame — head frame — $O_B X_B Y_B$ attached to the head in the point being in minimum allowable distance to driller (drilling point), or to the milling tool (for milling).

2) Non-moving frame — reference frame — $O_A X_A Y_A$ with origin attached to the center of the circle (hole).

The frame $O_B X_B Y_B$ undergoes translation and rotation with the tool displacement.

Three supporting heads are applied, where one is a non-moving, fixed support (no translation and rotation is possible), while the other two are mobile supports. Our aim is to create the plan of mobile head movements to provide satisfactory support for drilling and for milling.

In satisfactory support the distance c between the drilling (or milling) tool and the head edge is in the range (d_{min}, d_{max}) . The values of d_{min} , d_{max} depend on the operation requirements and can be different for drilling and milling.

length of edge equal to a . Figure 3 shows the applied notation.

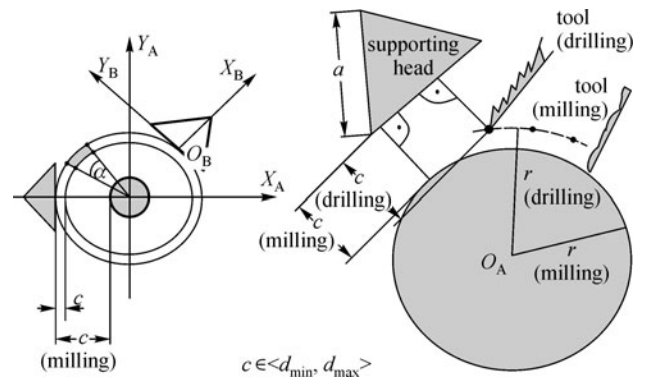


Fig. 3 Illustration of required conditions; c distances for drilling and milling are illustrative and not necessarily will keep the proportion used in figure (here c for milling is greater than c for drilling)

3.2 Basic considerations

3.2.1 Support by non-moving head

It is assumed that the supporting edge of the non-moving head is located symmetrically towards the frame $O_A X_A Y_A$ and the edge is parallel to the Y_A axis. The point in the middle of the edge is in the minimum allowable distance d_{min} from the drilling point. The orientation of $O_A X_A Y_A$ (and $O_B X_B Y_B$ accordingly) is the same. This assumption is taken for simplification of considerations without putting limits onto the generality of these considerations. First we evaluate how much of the edge (or how many drilled points) will be supported by a non-moving head, as the rest will need to be supported by moving heads. Based on Fig. 4 we have

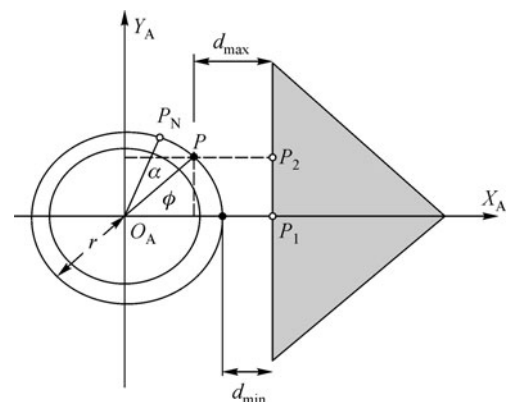


Fig. 4 Support by non-moving head

$$\begin{aligned} {}^A x_P &= r \cos \phi, \\ {}^A y_P &= r \sin \phi. \end{aligned} \tag{1}$$

The coordinates of points P_1 and P_2 are

$$\begin{aligned} {}^A x_{P_1} &= r + d_{\min}, \\ {}^A y_{P_1} &= 0, \end{aligned} \tag{2}$$

$$\begin{aligned} {}^A x_{P_2} &= r \cos \phi + d_{\max}, \\ {}^A y_{P_2} &= r \sin \phi. \end{aligned} \tag{3}$$

As can be seen in Fig. 4, ${}^A x_{P_1} = {}^A x_{P_2}$. Based on Eqs. (2) and (3), this results in

$$\begin{aligned} \cos \phi &= 1 + \frac{d_{\min} - d_{\max}}{r}, \\ \phi &= \arccos \left(1 + \frac{d_{\min} - d_{\max}}{r} \right). \end{aligned} \tag{4}$$

After obtaining ϕ , we will also know the value of ${}^A y_{P_2}$ by using Eq. (3). The angle 2ϕ marks an arc $2r\phi$ that is satisfactorily supported by the non-moving head. The supporting part of head edge has the length $2|P_1P_2|$ which means $2r|\sin\phi|$.

3.2.2 Support by moving heads

Displacements must be reduced to some appropriate amount.

We assume that for the drilling support a head follows the discrete tool path performing its motion in steps, where each step consists of a small displacement and rotation. For simplification we start taking into account the head position as it was for the non-moving case (the supported arc was evaluated above).

After the drilling is finished in point P (with d_{\max} distance to the edge), the head is translated by distance k_T along the X_A axis, hence the head edge crosses now the X_A axis in point P_T (Fig. 5). Then the head rotates by angle $(\phi + \alpha)$ and the drilling point P_N is now in distance d_{\min} from the head edge (Fig. 6).

$$\begin{aligned} {}^A x_{P_N} &= r \cos(\phi + \alpha), \\ {}^A y_{P_N} &= r \sin(\phi + \alpha), \end{aligned} \tag{5}$$

$$\begin{aligned} {}^A x_{P_3} &= (r + d_{\min}) \cos(\phi + \alpha), \\ {}^A y_{P_3} &= (r + d_{\min}) \sin(\phi + \alpha), \\ {}^A x_{P_T} &= \frac{r + d_{\min}}{\cos(\phi + \alpha)}, \\ {}^A y_{P_T} &= 0. \end{aligned} \tag{6}$$

Thus, it is obtained

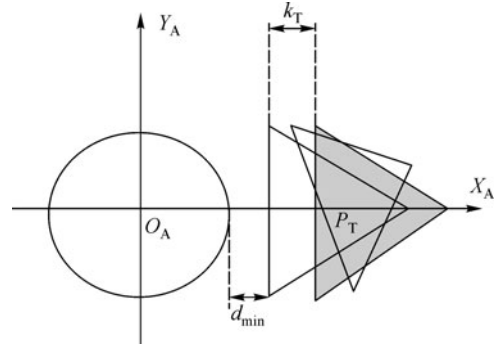


Fig. 5 At first the head is translated and next it is rotated

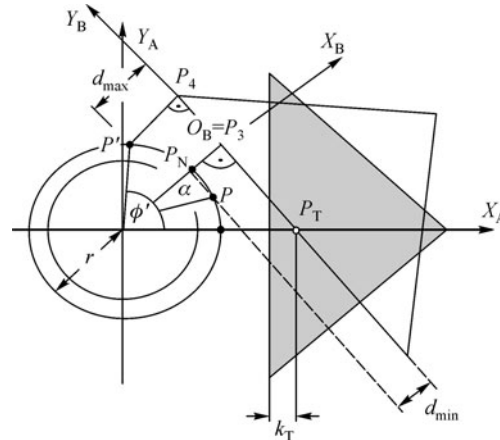


Fig. 6 Situation after one motion step

$$k_T = {}^A x_{P_T} - r - d_{\min} = \frac{r + d_{\min}}{\cos(\phi + \alpha)} - r - d_{\min}. \tag{7}$$

The above displacements can be iteratively repeated. The length of the head edge limits the number of repetitions. The final point P_F to be supported has the coordinate ${}^A y_{P_F} = (r + d_{\max}) \sin \theta_{\max} = 0.5a$. From this the maximum head rotation can be obtained, that means

$$\theta_{\max} = \arcsin \frac{0.5a}{r + d_{\max}}, \tag{8}$$

$$k_{T_{\max}} = {}^A x_{P_T} - r - d_{\min} = \frac{r + d_{\max}}{\cos \theta_{\max}} - r - d_{\min}. \tag{9}$$

3.3 Support with continuous head adjustment

3.3.1 Analysis of single head displacement

During milling, to provide a constant satisfactory distance to the milling point, the head moves in a way that its supporting edge rolls over an arc of the circle marking the

satisfactory supporting points. The radius of this circle is equal to r plus some distance within (d_{\min}, d_{\max}) . For clarity we shall assume that it is equal to $r + d_{\min}$. The head frame $O_B X_B Y_B$ is attached to point $P_i = P_{\min}$ being in minimum distance to the machined point ($O_B = P_1$ in Fig. 4 and $O_B = P_3$ in Fig. 6) and it continuously changes position and orientation in accordance with the tool motion.

The tool moves with a constant velocity v along an arc, which means that the point O_B moves along an arc of the circle $r + d_{\min}$. Let t be the time measured from beginning of tool motion starting from the point on the axis X_A (this determines orientation of non-moving frame $O_A X_A Y_A$). Then the distance completed in time interval t by the tool along an arc is vt and the internal angle measured from initial position to current tool position is $\phi(t)$ (within the range $[-\pi/2, \pi/2]$) (Fig. 7). The coordinates of O_B expressed in frame $O_A X_A Y_A$ are

$$\begin{aligned} {}^A x_{O_B} &= (r + d_{\min}) \cos \phi(t), \\ {}^A y_{O_B} &= -(r + d_{\min}) \sin \phi(t). \end{aligned} \quad (10)$$

To calculate the coordinates of some reference point ${}^A P_i$ when ${}^B P_i$ is known, we apply the homogenous transformation matrix:

$${}^A_B \mathbf{T} = \begin{bmatrix} \cos \phi(t) & -\sin \phi(t) & (r + d_{\min}) \cos \phi(t) \\ \sin \phi(t) & \cos \phi(t) & (r + d_{\min}) \sin \phi(t) \\ 0 & 0 & 1 \end{bmatrix}, \quad (11)$$

Then,

$${}^A \mathbf{P}_i = {}^A_B \mathbf{T} {}^B \mathbf{P}_i. \quad (12)$$

This can be used for example, to evaluate the coordinate of point ${}^A P_T$ (Fig. 6) as

$${}^B \mathbf{P}_T = \begin{bmatrix} 0 \\ -(r + d_{\min}) \phi(t) \\ 1 \end{bmatrix},$$

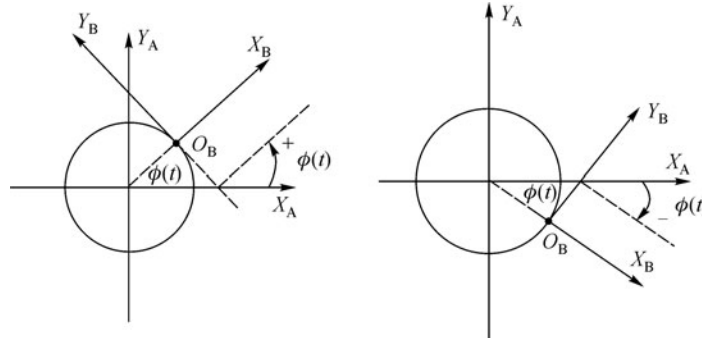


Fig. 7 Displacements of frame $O_B X_B Y_B$

$$\begin{aligned} {}^A x_{P_T} &= \sin \phi(t) (r + d_{\min}) \phi(t) + (r + d_{\min}) \cos \phi(t), \\ {}^A y_{P_T} &= -\cos \phi(t) (r + d_{\min}) \phi(t) + (r + d_{\min}) \sin \phi(t). \end{aligned} \quad (13)$$

Similar formalization can be applied for drilling when there is a constant distance from the head edge to each of the drilling points. In this situation, instead of the angle $\phi(t)$ given in the above formula, an angle ϕ_i must be used, which is the internal angle marking the position of i^{th} drilled point. Instead of a continuous head “rolling”, assumed in milling, the head changes its position in steps adjusting properly to the current ϕ_i . For head positioning it is sufficient to know the coordinates of ${}^A O_B$ and ${}^A P_T$, known from Eqs. (10) and (13), and the length of an arc $\phi(r + d_{\min})$ or $\phi(r + d_{\max})$, which will be explained. This distance is measured from the middle of the head edge to point O_B .

3.3.2 Final motion plan for moving heads

Each head starts its support by the corner and then “rolls” over the virtual circle marking the satisfactory support. The non-moving frame $O_A X_A Y_A$ is separately defined for each head currently fulfilling the support. The orientation of this frame is such that the X_A axis crosses the middle of the supporting edge for such head position when the middle point is considered as the supporting one (Fig. 4 — point P_1). This is for the head position denoted by 2 in Fig. 8(a). The initial position of the head is denoted by 2 and the last one by 3 (the grey triangle). When one head is performing the support, the next one moves to its initial supporting position. To avoid the obstruction between the neighboring heads, the next head will “roll” over a circle with a radius different from the previous one, which can be $r + d_{\max}$ as shown in Fig. 8(b).

3.4 Support with discrete head adjustment — introduction

The last analysis deals with the situation when the supporting head does not move during the machining of

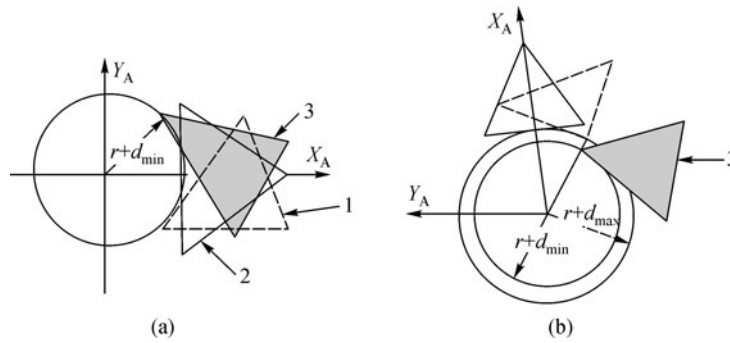


Fig. 8 Motion plan

supported fragment. The next head must be placed properly to support the next fragment. In Fig. 4, the current supporting head is marked by grey color and the next one is white. We will analyze the head positioning for proper support of the machined hole depending on the hole’s radius r . The orientation of frame $O_A X_A Y_A$ is determined by the localization of the currently supporting head. The origin of frame $O_A X_A Y_A$ is always in the middle of the machined hole and orientation is such that the positive part of X_A axis crosses the head edge in the point being in minimum allowable distance to the machined point (it is the head vertex P_1 in Fig. 9). The frame $O_B X_B Y_B$ is attached to the next supporting head in the point being in minimum allowable distance from the machined point and its orientation is such that the axis Y_B overlaps with the head supporting edge directing towards the machining direction. In Fig. 9 the next head is located in such a way that the frame $O_B X_B Y_B$ is attached also to the vertex (in the next head). The part supported by the edge of each head is illustrated in Fig. 4, the angle ϕ is given by (4) and α results from the drilled holes distribution (for drilling) or from the

required heads separation (for milling). If such separation is not needed α is set to zero. To shorten the description we will use $\beta = \phi + \alpha$. The rotation of frame $O_B X_B Y_B$ towards the previous frame $O_A X_A Y_A$ is β and translation is as given above. The values of d_{min} and d_{max} towards r are expected to be small therefore the angle β will be not be big. It must be checked if the proposed head placement will result in lack of head overlapping, which means the distance e marked in Fig. 9 must be more than zero.

For ease of calculations we will check first the distance from the head corner P_c to the axis X_A ; if this distance is satisfactory then the distance e between the corner of the previous head and the edge of next one will also be acceptable as shown in Fig. 9. The coordinates of point ${}^B P_c$ are

$$\begin{aligned} {}^B x_{P_c} &= a \sin(\pi/3), \\ {}^B y_{P_c} &= a \cos(\pi/3). \end{aligned} \tag{14}$$

The matrix ${}^A_B T$ is given by Eq. (11) (with the angle β). Multiplying matrix by vector ${}^B P_c$ obtains,

$$\begin{aligned} {}^A x_{P_c} &= \cos\beta {}^B x_i - \sin\beta {}^B y_i + (r + d_{min}) \cos\beta, \\ {}^A y_{P_c} &= \sin\beta {}^B x_i + \cos\beta {}^B y_i + (r + d_{min}) \sin\beta. \end{aligned} \tag{15}$$

To analyze possible overlaps, it will be easier to check the coordinates of the previous head in the new frame ($O_B X_B Y_B$); therefore, the following relationship obtained from Eq. (15) can be useful,

$$\begin{aligned} {}^B x_i &= \cos\beta {}^A x_i + \sin\beta {}^A y_i - (r + d_{min}), \\ {}^B y_i &= -\sin\beta {}^A x_i + \cos\beta {}^A y_i + p_1 \sin\beta - p_2 \cos\beta, \end{aligned} \tag{16}$$

where $p_1 = (r + d_{min}) \cos\beta$, and $p_2 = (r + d_{min}) \sin\beta$.

For lack of overlapping ${}^A x_{P_c}$ must be smaller than $r + d_{min}$ if ${}^A y_{P_c}$ is smaller than a . Or the example values (in $[m^{-3}]$) $d_{min} = 1$, $d_{max} = 10$, $r = 300$ and $a = 300$, it was obtained $\beta = 14.060^\circ$, ${}^B x_{P_c} = 259.8$, and ${}^B y_{P_c} = 150$ which results in ${}^A x_{P_c} = 507.5$, and ${}^A y_{P_c} = 280$. This means that the heads will overlap and a discrete placement plan is here impossible.

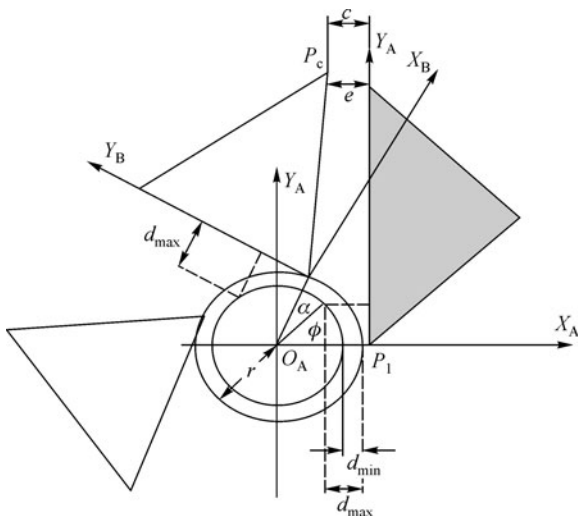


Fig. 9 Placement of heads for discrete motion

3.5 Support with discrete head adjustment — generalization

The machining begins with the initial position of the head as shown in Fig. 4. Two possible head placements are proposed. In the first one, point P_p of the head vertex is located on an arc of the circle with the radius $r + d_S$ ($d_{\min} < d_S < d_{\max}$),

$$\begin{aligned} {}^A x_{P_p} &= (r + d_S) \cos \phi, \\ {}^A y_{P_p} &= (r + d_S) \sin \phi, \end{aligned} \quad (17)$$

(ϕ is obtained using Eq. (4)) as shown in Fig. 10. In the second one, the coordinates of the vertex point P'_p are as follows (Fig. 11).

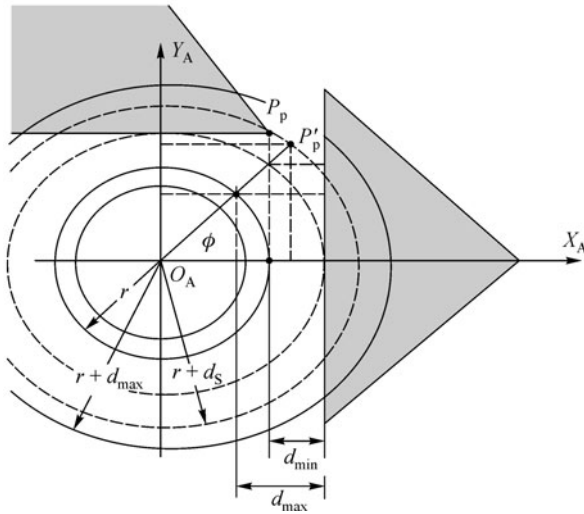


Fig. 10 Head corner placed in point P_p Eq. (17)

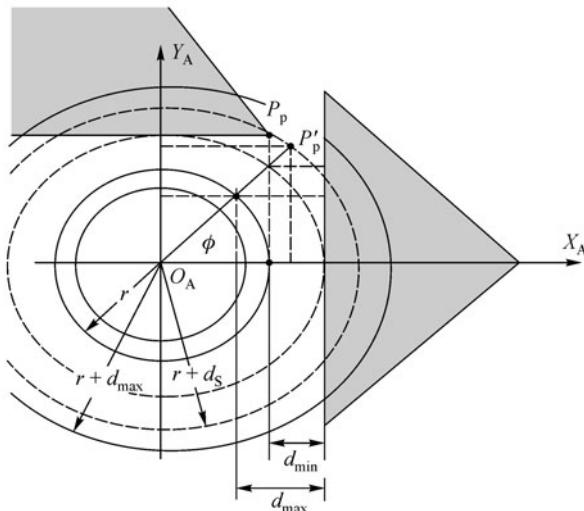


Fig. 11 Head corner placed in point P_p (Eq. (18))

$${}^A x_{P'_p} = (r + d_S) \cos \phi, \quad (18)$$

$${}^A x_{P'_p} = (r + d_{\min}) \tan \phi.$$

The supporting edge of the next head is tangent to the circle $r + d_{\min}$, which means that the frame $O_B X_B Y_B$ is rotated towards the frame $P_p X_c Y_c$ (or $P'_p X_c Y_c$, respectively) by the angle

$$\phi_0 = a \cdot \cos \left((r + d_{\min}) / d \right), \quad (19)$$

where d is the distance from the center of the hole to point $P_p(P'_p)$ as shown in Fig. 12.

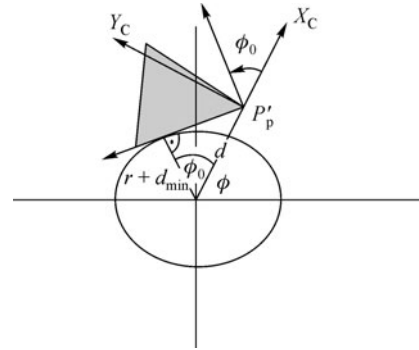


Fig. 12 Illustration of frame rotation angle ϕ_0

If the hole's radius is much bigger compared to the head size, then the end of the edge will end before the distance d_{\max} is reached (shown in Fig. 4). This is when $(r + d_{\min}) \tan \phi > {}^A y_{P_c}$ (not shown in Fig. 11), the distance d in Eq. (19) is now between O_A and P_c .

The origin of frame $O_B X_B Y_B$ has coordinates ${}^A x_{O_B} = (r + d_{\min}) \cos(\phi + \phi_0)$, and ${}^A y_{O_B} = (r + d_{\min}) \sin(\phi + \phi_0)$. To shorten the description we use $\gamma = \phi + \phi_0$. The transformation matrix is

$${}^A_B T = \begin{bmatrix} \cos \gamma & -\sin \gamma & {}^A x_{O_B} \\ \sin \gamma & \cos \gamma & {}^A y_{O_B} \\ 0 & 0 & 1 \end{bmatrix}. \quad (20)$$

With the transformation matrix given by Eq. (20), the coordinates of characteristic points (e.g., head edges) given in frame $O_B X_B Y_B$ can be easily expressed in frame $O_A X_A Y_A$.

$${}^A P_i = {}^A_B T {}^B P_i. \quad (21)$$

This results in

$$\begin{aligned} {}^A x_{P_i} &= \cos \gamma {}^B x_i - \sin \gamma {}^B y_i + {}^A x_{O_B}, \\ {}^A y_{P_i} &= \sin \gamma {}^B x_i + \cos \gamma {}^B y_i + {}^A y_{O_B}. \end{aligned} \quad (22)$$

The relations transforming to frame $O_B X_B Y_B$ are

$$\begin{aligned} {}^B x_i &= \cos \gamma^A x_i + \sin \gamma^A y_i - (r + d_{\min}), \\ {}^B y_i &= -\sin \gamma^A x_i + \cos \gamma^A y_i + {}^A x_{O_B} \sin \gamma - {}^A y_{O_B} \cos \gamma. \end{aligned} \quad (23)$$

When transforming the coordinates of the head vertices, we must take into account that $P = P'_p$, $P = P_p$ or $P = P_c$ depends on given situations.

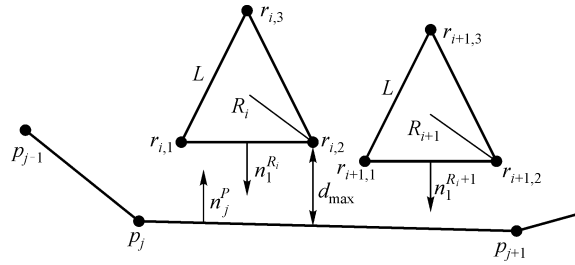


Fig. 13 Geometric constraints for head placement

4 Feasible head placement for milling polygonal contour

4.1 Geometric description

We assume that the workpiece contour is modeled as a two-dimensional (2D) simple closed polygonal chain with a given number of linear segments. Closed polygonal curve P in 2D space is described as the ordered set of vertices

$$P = \{p_1, \dots, p_{M+1}\} = \{(x_1, y_1), \dots, (x_{M+1}, y_{M+1})\}, \quad (24)$$

where the last vertex coincides with the first one, i.e., $p_{M+1} = p_1$. The workpiece boundary consists of M line segments. Each line segment can be described by the following equation:

$$y = a_j x + b_j, \quad j = 1, \dots, M. \quad (25)$$

The coefficients a_j and b_j of the line are calculated from the coordinates of the end points p_j and p_{j+1} :

$$\begin{aligned} a_j &= \frac{y_{j+1} - y_j}{x_{j+1} - x_j}, \\ b_j &= y_j - a_j x_j. \end{aligned} \quad (26)$$

Hereafter, both heads are assumed to be identical. The head R is an equilateral triangle

$$R_i = \{r_1, \dots, r_4\}, \quad (27)$$

where $r_4 = r_1$. Edge length of the triangle is equal to L .

We assume that the head configuration is specified by $q = (x, y, \theta)^T$, where x, y are Cartesian coordinates relative to a fixed reference coordinate frame and θ is the orientation angle. Configuration space (C-space) of the head is $Q = \mathbb{R}^2 \times S^1$, where S^1 is the unit circle. Moreover, we explicitly represent the normal vectors for each edge of the head and line segment of the part contour. We denote these normal vectors by $n_k^{R_i}$ for the normal to edge k of the head location i and n_j^P for the normal to j line segment of the polygonal curve P . It should be noted that the head edges depend on the orientation θ (but not on x, y -coordinates). Figure 13 shows the geometric constraints.

4.2 Constraints

Four main conditions need to be satisfied for every admissible head placement, R_i :

- 1) The biggest distance between the head and the working profile (workpiece contour) has to be d_{\max} to avoid vibrations during contouring.
- 2) The head surface must not come in contact with the tool.
- 3) The maximum allowable distance between the two subsequent head locations has to be d_{\max} .
- 4) The heads must not overlap each other.

To satisfy these conditions we must know the minimum and maximum distance between the two objects. Minimum distance calculation is essential for collision detection; if the minimum distance between the two objects is zero, then they are in contact. The distance between the two polytopes (in 2D polygons) Q and P is defined as

$$d_m(P, Q) = \min_{p \in P, q \in Q} \|p - q\|. \quad (28)$$

Equation (28) can be reformulated in terms of the Minkowski difference of the two polytopes, i.e.,

$$P \ominus Q = \{z | z = p - q, p \in P, q \in Q\} = Z. \quad (29)$$

Using Eq. (29), Eq. (28) can be rewritten as

$$d_m(P, Q) = \min_{p \in P, q \in Q} \|p - q\| = \min_{z \in P \ominus Q} \|z\|. \quad (30)$$

and we have reduced the problem of computing distance between the two polytopes to the problem of computing the minimum distance from one polytope to the origin of the coordinate frame. The Minkowski difference of two convex polytopes is itself a convex polytope. Because $Z = P \ominus Q$ is a convex set, and because the norm, $\|z\|$, is a convex function, $\hat{z} = \arg \min_{z \in Z} \|z\|$ is unique. However, p and q to achieve this minimum are not necessarily unique. To compute the minimum distance, the well-known GJK algorithm [11] is used.

The Euclidean distance d from point $p_k = (x_k, y_k)^T$ to the line segment $y = a_j x + b_j$ can be calculated by the following expression:

$$d = \frac{|y_k - a_j x - b_j|}{\sqrt{1 + a_j^2}} \quad (31)$$

The largest allowable distance between the head and the working profile has to be d_{\max} to avoid vibrations during contouring

$$d_i(P, R_i) \leq d_{\max}, \quad i = 1, \dots, N-1. \quad (32)$$

This means that the distance between the workpiece contour and the closest edge $E_k^{R_i}$ of the head R_i to the contour segment must not be larger than d_{\max} . The heads must not overlap each other,

$$\text{int}(R_i) \cap \text{int}(R_{i+1}) = \emptyset, \quad i = 1, \dots, N-1, \quad (33)$$

where $\text{int}(R_i)$ denotes the interior of the triangle. However, two heads may contact each other. Contact between the two heads can occur only when the orientation θ satisfies the following condition

$$\begin{aligned} (r_{i,j-1}(\theta_i) - r_{i,j}(\theta_i)) \cdot n_k^{R_{i+1}}(\theta_{i+1}) &\geq 0, \\ (r_{i,j+1}(\theta_i) - r_{i,j}(\theta_i)) \cdot n_k^{R_{i+1}}(\theta_{i+1}) &\geq 0, \\ j, k &= 1, 2, 3; \quad i = 1, \dots, N-1. \end{aligned} \quad (34)$$

If this condition is satisfied there is contact between the edge, $E_k^{R_{i+1}}$, of head R_{i+1} and the vertex $r_{i,j}$ of head R_i . At one extreme, the vertices $r_{i,j}$ and $r_{i+1,k}$ coincide, while at the other extreme, vertices $r_{i,j}$ and $r_{i+1,k+1}$ coincide.

Similarly, when the condition

$$\begin{aligned} (r_{i+1,j-1}(\theta_{i+1}) - r_{i+1,j}(\theta_{i+1})) \cdot n_k^{R_i}(\theta_i) &\geq 0, \\ (r_{i+1,j+1}(\theta_{i+1}) - r_{i+1,j}(\theta_{i+1})) \cdot n_k^{R_i}(\theta_i) &> 0, \\ j, k &= 1, 2, 3; \quad i = 1, \dots, N-1, \end{aligned} \quad (35)$$

is satisfied there is a contact between the edge, $E_k^{R_i}$, of head R_i and the vertex $r_{i+1,j}$ of head R_{i+1} . At one extreme, vertices $r_{i+1,j}$ and $r_{i,k}$ coincide, while at the other extreme, vertices $r_{i+1,j}$ and $r_{i,k+1}$ coincide. The head surface must not come in contact with the tool

$$d_i(P, R_i) \geq d_{\min}, \quad i = 1, \dots, N. \quad (36)$$

5 Initial head configuration

For the optimization approach described above, it is essential to start with a well selected initial configuration of heads. This task includes searching for the proper number of heads and their placements, which satisfy the necessary conditions of neither having mutual coincidences nor crossing the workpiece contour. In this section we describe this initialization algorithm and illustrate its results for two contour workpieces.

The head initialization algorithm can be split into three sequential stages: 1) contour segmentation, 2) start- and breakpoint detection, and 3) head set placement for every contour segment.

5.1 Contour segmentation

The contour of the workpiece, which is the expected outcome of the milling process, is analyzed with the aim of decomposing it into line segments and vertices. A vertex marks a rapid change of the contour's curvature within a sufficiently large contour part. The second condition induces that two consecutive vertices should be separated by a sufficient distance. In this way we avoid contour segments with lengths below a head's side length. Each line segment is terminated by two consecutive vertices. In practice we expect the length of a line segment to be at least 70 mm (the side length of the head).

The vertices and the segments are classified into several classes. We have worked out different head positioning scenarios, depending on the class of the given line segment and its vertices (Fig. 14):

1) The average curvature of a line segment allows its classification into straight, nearly straight, convex or concave;

2) The vertex type is induced by the angle value at which two tangential lines (at two segments meeting at this vertex) cross. We distinguish: type 1: $\alpha < 60^\circ$, type 2: $60^\circ \leq \alpha < 90^\circ$, type 3: $90^\circ \leq \alpha < 120^\circ$, type 4: $120^\circ \leq \alpha < 165^\circ$, type 5: $165^\circ \leq \alpha < 180^\circ$, and type 6: $\alpha \geq 180^\circ$.

The line type is considered in the third stage of the initialization procedure, while vertex types are already important for the second stage.

5.2 Start-end breakpoints

Among the vertex classes the first two are important in this stage. A vertex of type 1 (its corresponding angle is less than 60°) will cause a failure of the placement plan, as we will not be able to position the head close enough to the first segment of this vertex and not allowing the head to cross the second segment of this vertex. Hence, this vertex type induces a breakpoint for our head placement procedure- we need to make it as start/end point in the third stage. If more than one such vertex exist then the first one marks a start/end point whereas the other are breakpoints. In the latter case, two or more independent head placement plans will be searched for.

With no vertices of type 1 detected in the contour, we are happy to apply a vertex of type 2 as a starting point (with an angle slightly more than 60°). Such a vertex is ideally suited for a single head placement with a limited number of alternatives. Hence, the chance to revise the start head placement anytime later will be very low.

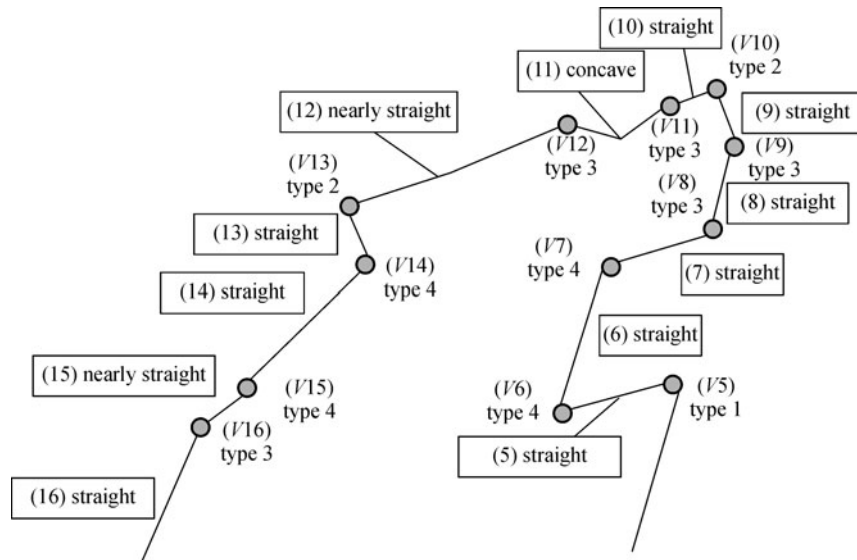


Fig. 14 Illustration of contour segmentation into line segments and vertices

5.3 Head set placement

In this stage, a head set placement is performed iteratively for every segment, one after the other.

5.3.1 Positioning at vertices

The head location starts with the segment determined either by the “failure” vertex of type 1 or by the most perfect vertex of the contour, i.e., an angle of type 2. Different scenarios of the head placement are needed depending on the vertex type (Fig. 15). A vertex of type 1 puts no further constraints onto the head placement. We treat it as an end vertex of the given line segment and start the placement process at the other end of this segment. A vertex of type 2 induces a single head to be in central position on the symmetry axis of tangential lines. The neighborhood of a vertex of type 3 is covered by two heads, where one is placed along one side whereas the second one completes the vertex area as much as possible. The area of a vertex of type 4 is well suited to be filled by two heads, located symmetrically with respect to the corresponding angle’s symmetry axis. A vertex of type 5 induces 3 heads, where the second is located in the central place on the angle’s symmetry axis. A vertex of type 6 induces no specific constraints.

5.3.2 Positioning at segments

Having located the heads at two vertices terminating given line segment, additional head positions are determined along the line segment to match the two border positions (Fig. 16). In this way we determine the number of required heads that are located sufficiently close to each other. The

type of line determines whether the orientation of consecutive heads is step-by-step changed or not. In the given example we observe a convex line segment that is matched by 4 heads. Two of them are placed at vertices (t_1 and t_4), while the two others build the interior part. Their orientations change from start- to end-head. The initial head placements for two workpieces are shown in Figs. 17 and 18.

The first contour consists mainly of large-sized linear segments that cause no serious difficulties for the head initialization procedure. The blank-circle-marked vertex candidates were omitted, because they are at a small distance to “dominating” vertices. The second contour is more difficult to process because it consists of many small line segments and the contour’s orientation changes rapidly many times. Again some green-points were filtered out to avoid small-size segments. This is an open contour, and we start it at the right end. Although the initial point is a “virtual” vertex only, the second end of this first segment is represented by a vertex of type 2, which plays the role of a start vertex.

6 Numerical results

Proposed solutions were tested using the programs written in MATLAB. The heads with the edge length equal to 70 mm as it will be used in the real test bed were considered. The most typical circular holes in the machined parts have a radius of 75 mm. Those holes were first taken into account in the analysis. The holes of smaller and bigger radiuses were also considered. The minimal and maximal distances are determined by machined material properties and are equal to $d_{\min} = 1$ mm, $d_{\max} = 10$ mm.

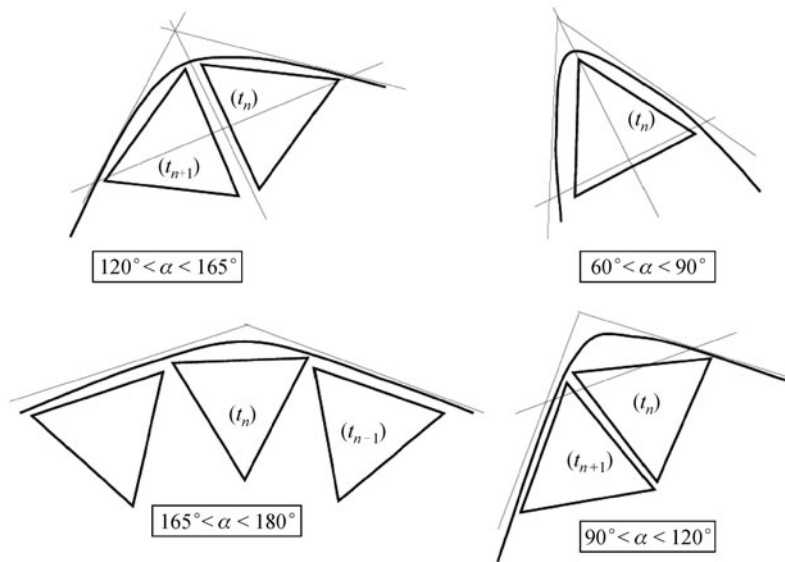


Fig. 15 Positioning at vertices

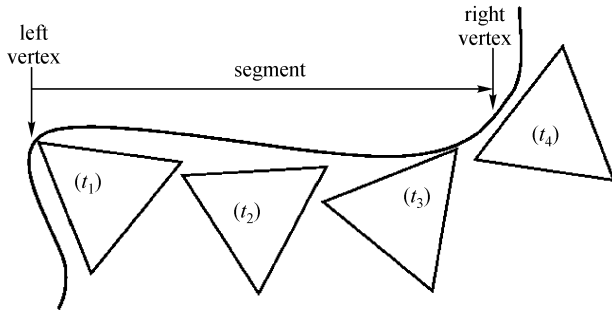


Fig. 16 Positioning along line segments

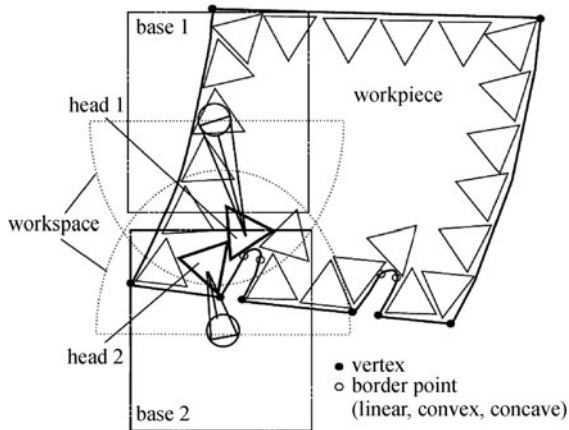


Fig. 17 Head location plan for workpiece 1

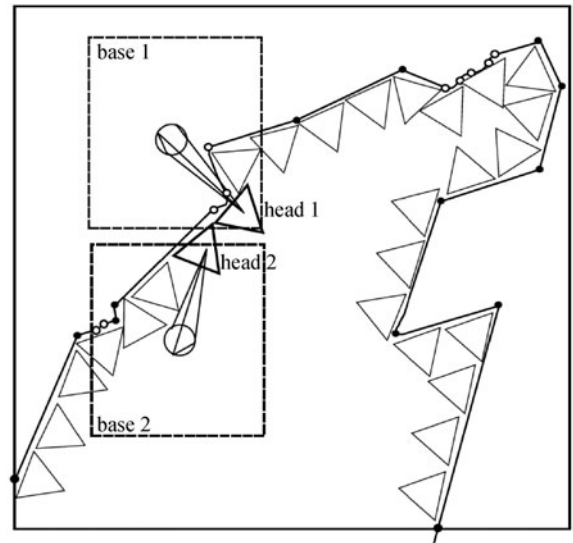


Fig. 18 Head location plan for workpiece 2

Figure 19 shows the result obtained for the head placement given in Fig. 9. Each head supports the arc with an internal angle of 28.3576° . To avoid overlapping of

the heads, the added angle α must be more than 6° . With $\alpha = 6^\circ$ the next and previous head are in contact. This means that this head arrangement can be used only when the internal angle for consecutive drilling points is more than 6° . With the angle $\alpha = 7.6424^\circ$ the support by 10 head positions is obtained.

In the next tests the discretized head placement as described in generalization was analyzed. First $d_S = 0.5d_{max}$ was taken into account. With $r = 75$ the non-moving head located as shown in Fig. 4 supports the arc with an internal angle of 56.7153° . If the moving heads corner coordinates are given by Eq. (17), each moving head supports the arc with the internal angle of 44.8506° .

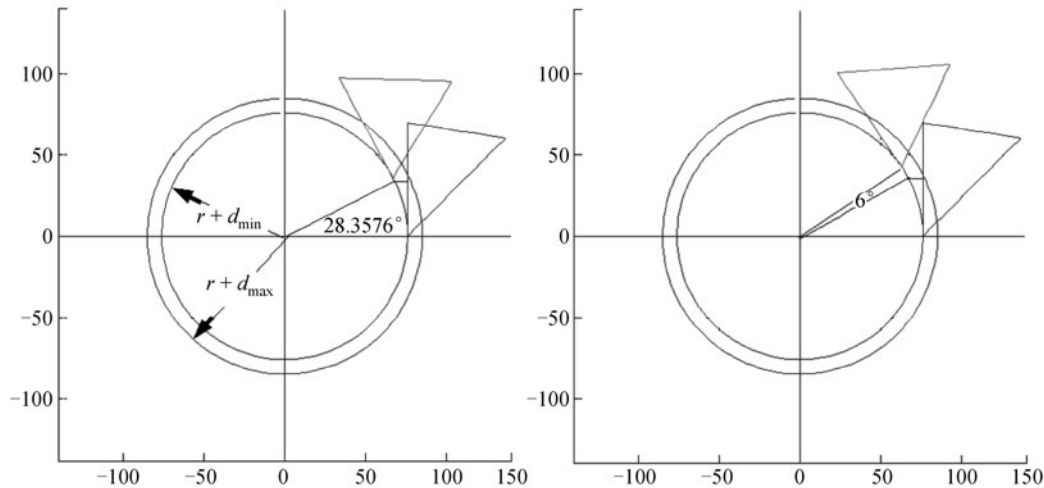


Fig. 19 Picture obtained with first head planning program—size proportions are kept

This means that 6.7621 of the moving heads is needed to support the whole arc. For the moving heads corner coordinates given by Eq. (18) each moving head supports the arc with the internal angle of 44.2875° . This means that 6.8481 of the moving heads is needed to support the whole arc.

The number of heads must be an integer, which means that with 6 heads a significant part of the arc will be not supported (e.g., 0.7153 of the head edge is 50.0710 mm).

The satisfactory solution was obtained by decreasing d_S , which increased the head twist, decreased the angle supported by one head and increased the number of required heads. For this purpose the iterative optimizing program was written. d_S is decreased by small steps and the angles supported by moving head (also taking into account the non-moving head localization) are calculated. The program stops if the number of heads (including the non-moving one) supporting the whole hole exceeds the nearest but smaller integer by a very small value η . In our optimization η was set to 0.01 (this is equivalent to 0.7 mm). With $d_S = 0.43d_{\max}$ and Eq. (18), 7.0367 was obtained for movable heads. Applying 7 heads, we have unsupported (within the d_{\min} , d_{\max} limits) 0.0367 of the head edge (it is 2.569 mm). For $d_S = 0.44d_{\max}$, 7.0083 was obtained for movable heads (each supporting 43.2753°). The unsupported (within the d_{\min} , d_{\max} limits) 0.0083 of the head is equal to 0.581 mm. Figure 20 shows the solution, with the whole cycle the last movable supporting head (head position No. 7) does not overlap the non-moving head (head N).

In the next example, $r = 35$ was considered. The non-moving head supports the arc with an internal angle of 84° . For $d_S = 0.5d_{\max}$ with head corner coordinates chosen according to Eq. (17), each moving head supports the arc with an internal angle of 67.8666° . This means that 4.0668 of the moving heads is needed to support the whole arc.

With head corner coordinates given by Eq. (18) each moving head supports the arc with the internal angle 66.314° . This means that 4.162 of the moving heads is needed to support the whole arc.

The number of heads must be an integer as discussed, and with 4 heads some small part of the arc will not be supported. The missing part for 0.0668 is equal to 4.676 mm. The distance d_S was modified by the optimization program as done previously. For the difference the head corner coordinates given by Eq. (17) were taken into account. The satisfactory result was obtained for $d_S = 0.535d_{\max}$, when the moving head supports the arc with an internal angle of 68.8745° . This needs 4.0078 of the moving heads. With 4 heads the missing 0.0078 is equivalent to 0.546 mm, which fulfils the accuracy criterion.

7 Summary

This paper proposes a concept of a planner for a self adaptable, reconfigurable fixture system for thin-walled workpieces like sheet-metal parts with complex surface geometries. The fixture should be applicable to parts with different shapes as well as distributions and densities of holes, milled contours, and variously shaped openings. Two types of machining processes have been considered: drilling of various small holes and milling when making larger holes and contouring the workpiece. Based on CAD models of the parts and given geometric constraints two solutions for an admissible head placement for two reference parts with different geometry of the contour have been proposed. In the results, we obtain the sequence of the supporting heads that provide continuous support in close proximity to the tool. Future work will include the next phases of the planning process, namely planning a

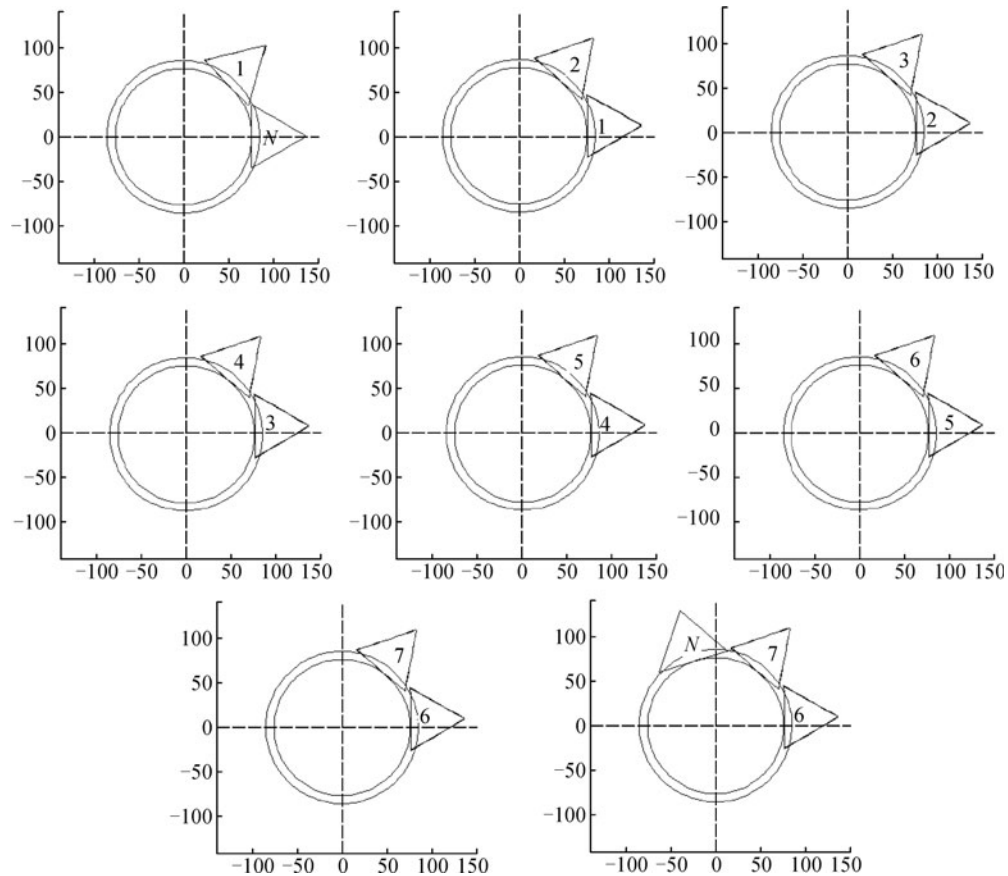


Fig. 20 Picture obtained with the optimization program—size proportions are kept

corresponding sequence of mobile bases locations, and trajectory planning for mobile bases and PKMs.

Acknowledgements This work was supported by the European Union Framework Program Theme (NMP-2007-3.2-1) within the Project SwarmIt-Fix (No. FP7-214678).

References

1. Menassa R, De Vries W. Optimization methods applied to selecting support positions in fixture design. *ASME Journal of Engineering for Industry*, 1991, 113(4): 412–418
2. Vallapuzha S, De Meter E C, Choudhuri S, Khetan R P. An investigation of the effectiveness of fixture layout optimization methods. *International Journal of Machine Tools and Manufacture*, 2002, 42(2): 251–263
3. Sela M N, Gaudry O, Dombre E, Benhabib B. A reconfigurable modular fixturing system for thin-walled flexible objects. *International Journal of Advanced Manufacturing Technology*, 1997, 13(9): 611–617
4. Shirinzadeh B, Tie Y. Experimental investigation of the performance of a reconfigurable fixture system. *International Journal of Advanced Manufacturing Technology*, 1995, 10(5): 330–341
5. Youcef-Toumi K, Liu W, Asada H. Computer-aided analysis of reconfigurable fixtures and sheet metal parts for robotics drilling. *International Journal of Robotics and Computer-Integrated Manufacturing*, 1988, 4(3–4): 387393
6. Bi Z M, Zhang W J. Flexible fixture design and automation: review, issues and future directions. *International Journal of Production Research*, 2001, 39(13): 2867–2894
7. Kang Y, Rong Y, Yang J, Ma W. Computer-aided fixture design verification. *Assembly Automation*, 2002, 22(4): 350–359
8. Cai W, Hu S J, Yuan J X. Deformable sheet metal fixturing: principles, algorithms, and simulations. *Transactions of ASME, Journal of Manufacturing Science and Engineering*, 1996, 8(3): 318–324
9. DeMeter E C. Fast support layout optimization. *International Journal Machine Tools and Manufacturing*, 1998, 38(10–11): 1221–1239
10. Rearick M R, Hu S J, Wu S M. Optimal fixture design for deformable sheet metal workpieces. *Transactions of NAMRI/SME*, 1993, 21: 407–412
11. Gilbert E, Johnson D, Keerthi S. A fast procedure for computing the distance between objects in three-dimensional space. *IEEE Journal of Robotics and Automation*, 1988, 4(2): 193–203